The Plant Journal (1996) **9**(4), 457–465

Tissue and intra-cellular distribution of coconut cadang cadang viroid and citrus exocortis viroid determined by *in situ* hybridization and confocal laser scanning and transmission electron microscopy

Roderick G. Bonfiglioli, Daryl R. Webb and Robert H. Symons*
Department of Plant Science, Waite Agricultural Research Institute, University of Adelaide, Glen Osmond, SA 5064, Australia

Summary

Confocal laser scanning microscopy and transmission electron microscopy (TEM) were used in conjunction with *in situ* hybridization techniques to compare and contrast the subnuclear (ultrastructural) and tissue (histological) localizations, respectively, of citrus exocortis viroid (CEV) and coconut cadang cadang viroid (CCCV). Both these viroids, which are members of the same taxonomic subgroup of viroids, were found in the vascular tissues as well as in the nuclei of mesophyll cells of infected host plants. At the subnuclear level, however, CEV was distributed across the entire nucleus, in contrast to CCCV which was mostly concentrated in the nucleolus with the remainder distributed throughout the nucleoplasm.

Introduction

Viroids are small single-stranded circular RNA molecules ranging in size from 246 to 371 nt in length. They are the smallest known pathogens of higher plants and many aspects of their biology are currently little understood. Comparative nucleic acid sequence data (Keese and Symons, 1985, Koltunow and Rezaian, 1989) have enabled a taxonomic classification of the viroids into two main groups, the potato spindle tuber viroid (PSTV) group and the avocado sunblotch viroid (ASBV) group. The PSTV group of viroids is further subdivided into three subgroups, the PSTV subgroup, the apple scar skin viroid (ASSV) subgroup and the coleus blumei viroid (CbV) subgroup.

Studies utilizing specific inhibitors of the nuclear RNA polymerases have indicated a role for RNA polymerase II, which is located in the nucleoplasm (Bregman *et al.*, 1995; Hendzel and Bazett-Jones, 1995) in the replication of viroids in the PSTV subgroup, including PSTV (Schindler and Mühlbach, 1992; Speismacher *et al.*, 1985) and CEV (Rivera-Bustamante and Semancik, 1989), but not in the synthesis of ASBV (Marcos and Flores, 1992). These findings are in general agreement with observations made from ultrastructural studies that show that some members of the PSTV subgroup, PSTV (Harders *et al.*, 1989) and CCCV, have been localized to the nucleus, while ASBV has been localized to the chloroplast (Bonfiglioli *et al.*, 1994).

The basis of host specificity for different viroids at the level of plant family or class has not been determined, but the host range of many viroids is known to vary. ASBV, for instance, has a narrow host range and is apparently restricted to members of the family Lauraceae (Da Graca and Van Vuuren, 1981), while PSTV and CEV are known to have a much broader host range among many dicotyledonous plants (Diener, 1979). CCCV is apparently restricted to the genus *Cocos* in the arecoid group of the Palms and, together with coconut tinangaja viroid (CTiV), they are the only two viroids known to be found in monocotyledonous plants (Boccardo *et al.*, 1981; Haseloff *et al.*, 1982; Keese *et al.*, 1987), while all other known viroids are restricted to dicotyledonous plants.

Little work has been done using microscopy to locate viroids within plants at the tissue level, but it is known that PSTV is found within the nucleolus of infected tomato (*Lycopersicon esculentum*) plant cells (Harders et al., 1989). Semancik and Vanderwoude (1976), and Wahn *et al.* (1980) used electron microscopy to examine the relationship between plasmalemmasomes and CEV infection. In an earlier paper (Bonfiglioli *et al.*, 1994), we located ASBV to the thylakoid membranes of chloroplasts from mesophyll cells of ASBV-infected avocado (*Persea americana*) plants and we localized CCCV to the nucleus of cells associated with the periphery of vascular bundles in fronds from CCCV-infected oil palms (*Elaeis guineensis*). Further analysis of the subnuclear distribution of CCCV in these cells showed that, while there was five times more total viroid in the nucleoplasm, there was actually a much higher concentration of the viroid within the nucleolus. It is known that plants can be systemically infected by inoculation with gel-purified viroid extracts from other infected plants (Semancik and Weathers, 1972) and this does suggest that they should be present, at least early in the infection process, in the vascular system. An accurate knowledge of the

Received 30 August 1995; revised 3 January 1996; accepted 12 January 1996.
*For correspondence (fax +61 8 303 7102).

localization of viroids at the tissue and the ultrastructural levels is important in viroid pathogenicity studies as well as in studies of replication strategies. There is very little knowledge on the pathogenic mechanisms of viroids and a fuller understanding of the basic biology of viroids is needed for this purpose.

Results

In this paper we have used viroid-specific cRNA probes in *in situ* hybridization experiments with confocal microscopy and TEM to localise the viroids CEV and CCCV at the tissue and subcellular levels. For confocal microscopy, we have used viroid-specific minus (–) sense (complementary) biotinylated cRNA probes to localize the dominant plus (+) sense form of the viroids CEV and CCCV. In order to avoid the problems caused by the high level of cellular autofluorescence seen in the red and green channels on the confocal microscope, we have used a far-red fluorochrome, Cy5, conjugated to strepavidin to localize the biotin moieties in the cRNA probes. We have used similar *in situ* hybridization methods in conjunction with TEM to further localize the viroids within the cells and to determine their exact subcellular localization. The biotin in these experiments was localized by 15 nm gold beads conjugated to strepavidin.

Both CEV and CCCV are found in the vascular tissues and in the mesophyll cells

In situ hybridization experiments with minus sense viroid probes in conjunction with confocal microscopy showed that both CEV and CCCV were found in the vascular tissues. Figure 1(a) shows leaf vascular tissue from CEV-infected tomato and the viroid signal is clearly seen in the vascular tissue. At higher magnification (not shown) it was possible to distinguish between the ribbed xylem vessels and the phloem cells, and the viroid signal was mostly confined to the phloem. Examination of multiple frames from each of 12 sections of infected leaf material showed that the viroid concentration in the leaves is consistently higher than in any other part of the plant examined. The healthy control sample of leaf vascular tissue shown in Figure 1(b) has no viroid signal. Figure 1(c) shows vascular tissue in a section from a root sample of CEV-infected tomato where the viroid signal is confined to a single line of vascular cells. Examination of multiple frames from each of 12 sections of root tissue showed that the viroid concentration in the roots is not as high as in the leaves. Other than vascular tissues, the only other tissue type that contained CEV was the mesophyll cells. Figure 1(d) shows the viroid located in the nucleus of a leaf mesophyll cell, the only cellular organelle to which we were able to locate the viroid in these cells.

CCCV was similarly located in the vascular system of CCCV-infected oil palm by confocal microcopy and *in situ* hybridization, as can be seen from Figure 2(a) and 2(b). Figure 2(a) shows that the viroid signal was at times seen in the cells on the periphery of the vascular bundle, while Figure 2(b) shows a more central location of the viroid within the middle of the vascular bundle. Figure 2(c) shows CCCV in the mesophyll cells with signal apparently in the nuclei. The healthy control samples, as for example, in Figure 2(d), showed no signal for CCCV in any tissues. The observations shown in these figures are typical observations from multiple frames from 12 sections of infected and healthy material. As for CEV, CCCV was not seen in other types of tissues, such as the palisade cells, but was very occasionally seen in the epidermal cells (Figure 2c).

CEV is distributed throughout the nucleus of tomato mesophyll cells

When *in situ* hybridization was used in conjunction with transmission electron microscopy, the subnuclear distribution of the viroid signal was easier to determine. Figure 1(f) is an electron micrograph of a CEV-infected tomato mesophyll cell and it shows that at this ultrastructural level the plus sense form of the viroid is distributed over the whole nuclear structure, and there is no concentration of the viroid in the nucleolus, although there do appear to be occasional concentrations of the viroid in patches throughout the nucleoplasm. Such concentrations in the nucleoplasm are more evident in the confocal microscopy image in Figure 1(d) and (e). This pattern of subnuclear distribution was the same in all sections examined. The same experiment conducted with the plus sense viroid probe (to localize

Figure 1. *In situ* hybridization to CEV in tomato.
(a) Confocal micrograph of branched vascular bundle (blue) from CEV-infected leaf tissue containing abundant CEV signal (red/orange).
(b) Confocal micrograph of vascular bundle (blue) and leaf mesophyll tissue (blue), healthy negative control.
(c) Confocal micrograph of CEV-infected root tissue from tomato (purple) showing viroid signal (green) in a single vascular thread.
(d) Confocal micrograph of single mesophyll cell from CEV-infected tomato leaf material showing cell nucleus with viroid signal (red/orange) and cell structure by auto fluorescence (green).
(e) Enlargement of nucleus from (d), shows viroid signal only in false colour intensity gradient (blue lowest level, pink-grey highest), image shows subnuclear distribution of viroid signal.
(f) TEM of mesophyll cell from CEV-infected tomato leaf material. *In situ* cRNA probes located by 15 nm gold beads (black dots) conjugated to strepavidin, viroid signal is spread through the nuclear structure.

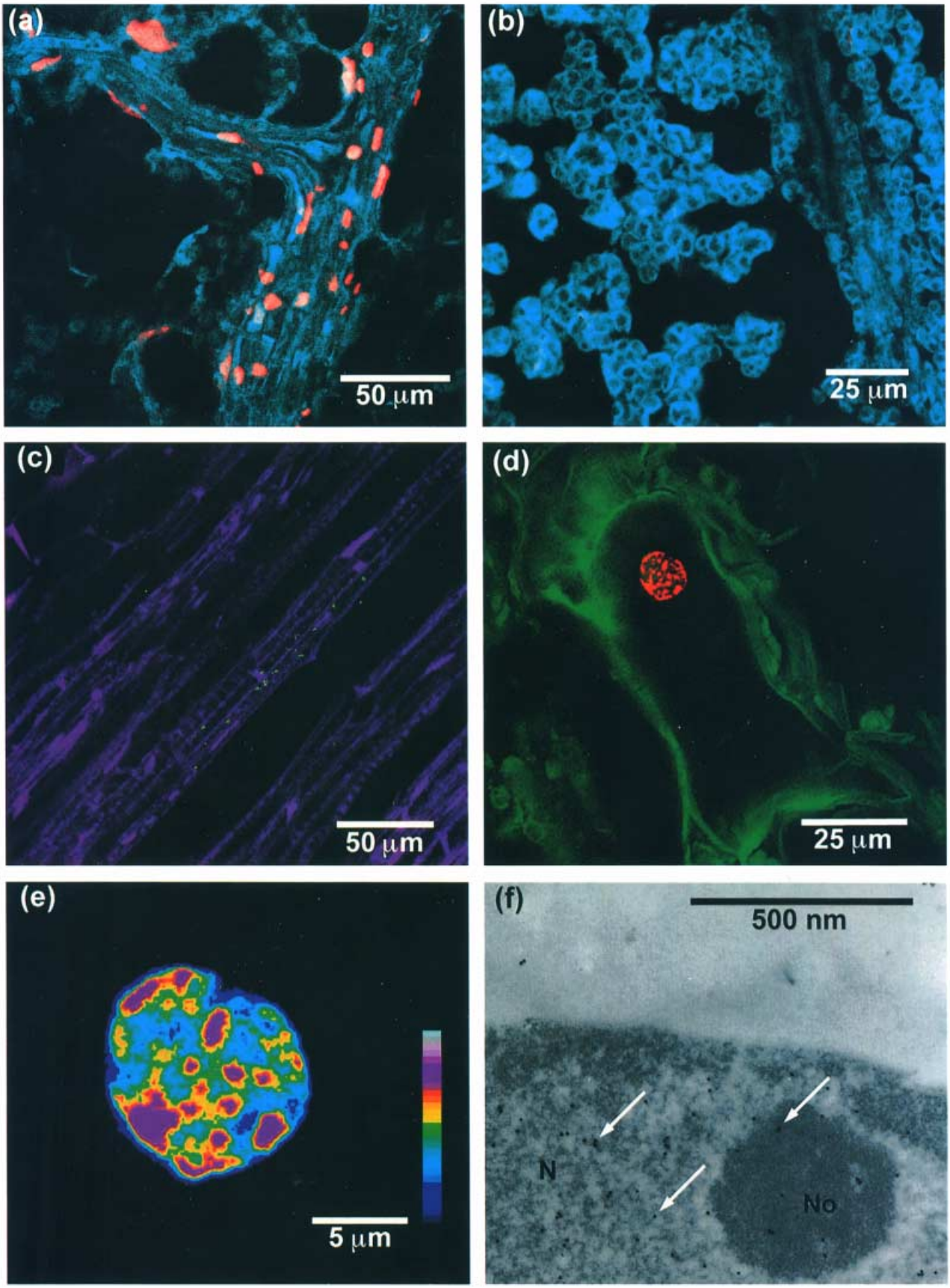
(a)
50 μm
(b)
25 μm
(c)
50 μm
(d)
25 μm
(e)
5 μm
(f)
500 nm
N
No

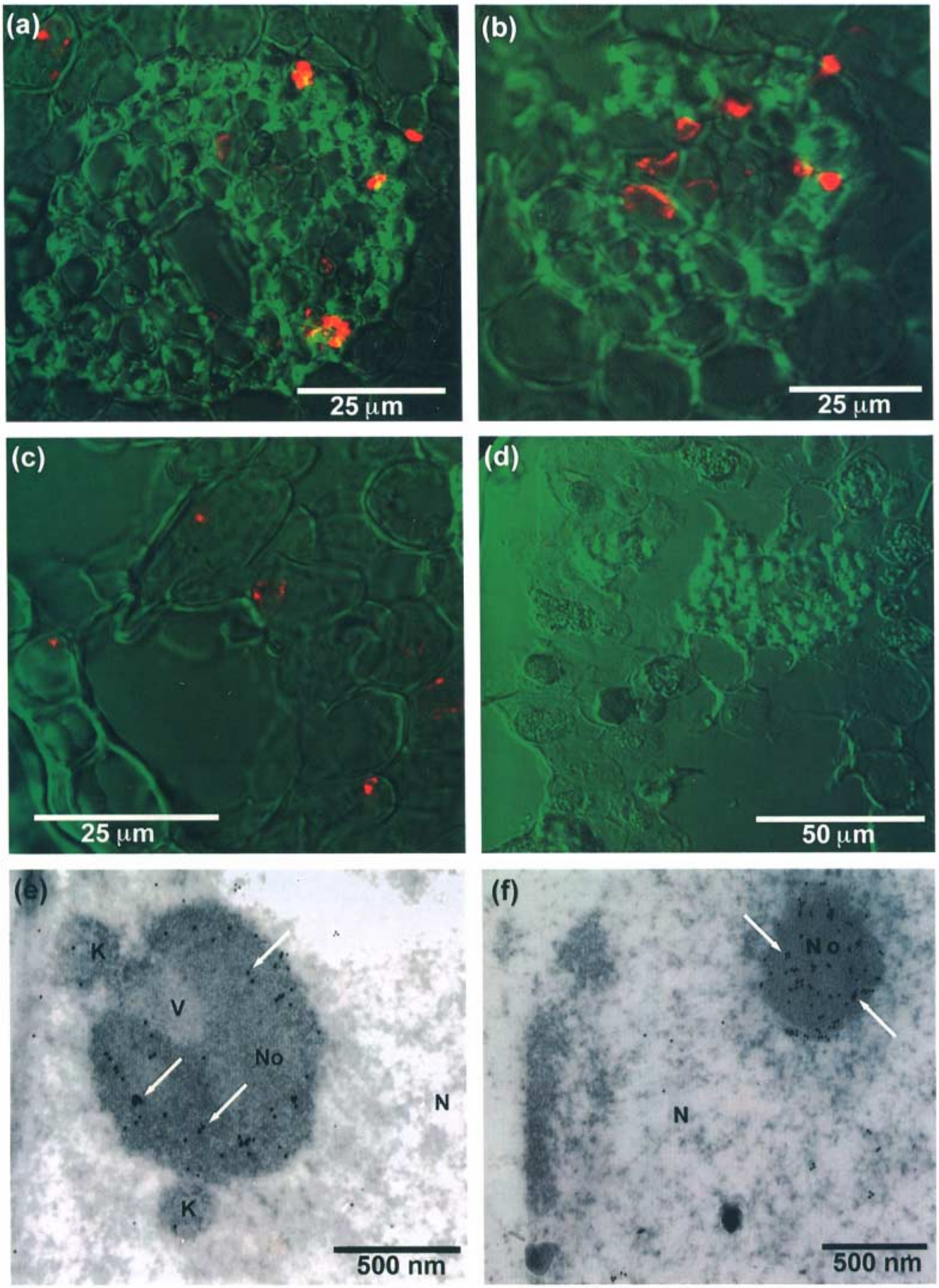
(a)
25 μm
(b)
25 μm
(c)
25 μm
(d)
50 μm
(e)
K
V
No
N
K
500 nm
(f)
No
N
500 nm

the minus sense viroids transcripts) showed a much weaker signal (data not shown) in the same location. Figure 1(e) is an enlargement of the nucleus seen in the confocal microscopy image of Figure 1(d) but with the viroid signal presented as a false-colour intensity gradient image; the viroid signal is, as in the electron micrograph of Figure 1(f), not specifically concentrated in the nucleolus, but is across the entire nuclear structure with localized concentrations in the nucleoplasm.

Time-course studies (with samples taken in duplicate weekly for 10 weeks, and with approximately 100 nuclei examined at each sampling) utilizing *in situ* hybridization and electron microscopy and designed to follow the progress of CEV infection in tomato have consistently shown that the viroid is distributed across the entire nucleus, with a gradual increase in the total amount, but with no change in the distribution of the viroid signal within the nuclear structure (data not shown).

CCCV is concentrated in the nucleolus of mesophyll cells of the oil palm

In situ hybridization experiments using minus strand probes for CCCV, and confocal microscopy showed that the plus form of the viroid was localized within the vascular bundles (Figure 2a and b), and also within the mesophyll cells (Figure 2c), where the viroid is found within the nuclei. Signal was observed in the samples taken from the new season fronds (2–3 months old), but not from younger tissue. The electron micrographs Figure 2(e) and 2(f) (Figure 2f reprinted from Bonfiglioli *et al.*, 1994) show that the viroid is mostly concentrated in the nucleolus, with the remainder distributed throughout the nucleoplasm (Bonfiglioli *et al.*, 1994). The signal at the ultrastructural level is often seen in the nuclei of cells on the edge of the vascular bundles which is consistent with the data from the confocal microscopy, as seen in Figure 2(a). The distribution of the viroid within the nucleolus was often towards the outer edge of the nucleolus, as seen in Figure 2(e). This concentration of the viroid in the nucleolus was a commonly seen pattern. Approximately 10 sections, comprising several hundred nuclei were examined, and 10–12% of those nuclei probed positive for CCCV, with 75% of them showing a clear concentration of viroids in the nucleoli. In the remaining nuclei the signal was not specifically concentrated in the nucleolus, but was spread throughout the nucleoplasm. The same experiments conducted with the plus sense viroid probe to localize the minus sense viroids showed a similar distribution of the viroid, but at a much lower incidence (data not shown). No signal was seen in sections from the healthy control plants (Figure 2d).

Avocado sunblotch viroid (ASBV) can be localized to the phloem, but not to the subcellular level, by confocal microscopy

Similar experiments to those described above have been carried out on the localization of ASBV using transmission electron microscopy (Bonfiglioli *et al.*, 1994) and confocal microscopy (data not shown). ASBV could be located within the vascular system of ASBV-infected avocado leaf tissue using confocal microscopy but, while we have previously localized ASBV at the ultrastructural level to the thylakoid membranes of the chloroplast using electron microscopy (Bonfiglioli et al., 1994), we have not been able to localize reliably ASBV to the subcellular level using confocal microscopy. This is possibly because the chloroplasts, which are effectively a compartment within the main cellular compartment, may not be as easily permeabilized by proteinase digestion as is the nucleus. Unlike the nucleus, chloroplasts have no pores (Kirk and Tilney-Bassett, 1978; Schnell and Blobel, 1993) to further assist the entry of probes and fluorochromes to their interiors. ASBV was not seen to be localized to any other cellular organelles or structures, and the healthy controls did not show any signal (Bonfiglioli *et al.*, 1994).

Discussion

In this paper we have used different types of microscopy in conjunction with nucleic acid hybridization techniques to localize unequivocally CEV and CCCV within the host tissues and at the ultrastructural level. We conducted our histological experiments (confocal microscopy) with only the minus sense cRNA viroid-specific probes to localize the more abundant plus form of the viroids, as earlier reports (Harders *et al.*, 1989) and our own earlier study

Figure 2. *In situ* hybridization to CCCV in oil palm.
(a) Confocal micrograph of cross-section of vascular bundle (green) from infected oil palm frond showing viroid signal (red) in peripheral cells of the bundle.
(b) Confocal micrograph of cross-section of vascular bundle (green) from infected oil palm showing viroid signal (red) in central cells of vascular bundle.
(c) Confocal micrograph of mesophyll cells (green) from infected oil palm showing viroid signal (red).
(d) Confocal micrograph of cross-section of vascular bundle with surrounding mesophyll tissue (green) from healthy control plant. No viroid signal is seen.
(e) TEM of nucleolus of CCCV-infected oil palm mesophyll cell. The viroid hybridization signal is located by 15 nm gold beads conjugated to strepavidin, shown by the white arrows. The signal is concentrated in the inner periphery of the nucleolus. (Reproduced from Bonfiglioli *et al.*, 1994.)
(f) TEM of cell nucleus from cell on periphery of vascular bundle. Hybridization signal is located with 15 nm gold beads (black dots) conjugated to streptavidin, viroid signal can be seen to be mostly concentrated within the nucleolus and only a low concentration in the nucleoplasm.
Abbreviations: No, nucleolus; N, nucleoplasm; V, central nucleolar vacuole; K, putative perinuclear knobs.

(Bonfiglioli *et al.*, 1994) have observed no differences between the locations of the plus and minus forms of the viroids, even at the subcellular level, using transmission electron microscopy. The latter experiments aimed at determining the ultrastructural localizations of the viroids and were conducted with both the plus and minus sense probes to confirm these observations.

At histological levels, the distribution and localization of the two viroids, at least in the plus form, appear to be similar; they are both found in the vascular tissues and in the mesophyll cells. The vascular localization is consistent with the observation that plants can be systemically infected by mechanical inoculation with purified viroid preparations via tomato cotyledons for CEV, or, in the case of CCCV infection of the oil palms used in this work, by stabbing and slashing the inoculum into the base of the stem. At the ultrastructural level, within the nuclei of the mesophyll cells, differences were seen in the subnuclear locations of the two viroids. CEV was distributed throughout the entire nuclear structure, while CCCV was mostly concentrated in the nucleolus. It was unexpected that two viroids from the same taxonomic subgroup should show different subnuclear distributions but, despite their close taxonomic grouping, these two viroids only share a 44% sequence homology (Keese *et al.*, 1988). It would be reasonable to consider then, that any differences in the ultrastructural localization between different viroids may reflect either differences in their methods of replication, or in how they exert their pathogenic effects.

It has been shown by studies using α-amanitin, an inhibitor of RNA polymerase II, that PSTV (Mühlbach and Sanger, 1979; Schindler and Mühlbach, 1992) and CEV (Rivera-Bustamante and Semancik, 1989) are both most likely transcribed by RNA polymerase II which is known to be located within the nucleoplasm (Bregman *et al.*, 1995; Hendzel and Bazett-Jones, 1995). Our time-course studies on CEV did not indicate any time-related factor in the subnuclear distribution of this viroid up to 10 weeks post-infection. The distribution of CEV was across the entire nucleus with scattered concentrations of viroid throughout the nucleoplasm and this finding is consistent with the localization of the large subfragment of RNA polymerase II, as described in Bregman *et al.* (1995). However, in a previous paper (Bonfiglioli *et al.*, 1994), we used *in situ* hybridization with transmission electron microscopy to localize CCCV at the ultrastructural level, and we found that CCCV was present at a much greater concentration in the nucleolus than it was in the nucleoplasm (see Figure 2f). If CCCV is replicated by RNA polymerase II in the nucleoplasm, as the evidence for other viroids in the PSTV subgroup so far indicates (Rivera-Bustamante and Semancik, 1989; Schindler and Mühlbach, 1992), then how, or why, it should become concentrated in the nucleolus is an important question, the answer to which may shed some light on the pathogenic mechanism of this and other viroids. The other, and more simple explanation, however, is that CCCV is replicated in a monocot host by RNA polymerase I, a nucleolar enzyme (Scheer and Rose, 1984), and that the viroids found in the nucleoplasm have moved there after replication in the nucleolus.

It is tempting to speculate that the differences in the ultrastructural locations observed between CEV and CCCV in our study might be due to differences in the host plants (monocots versus dicots), but the PSTV studies by Harders *et al.* (1989) where PSTV was found to be localized in the nucleolus were also done using tomato, which is the same host plant we used in our studies where CEV was found to be spread across the entire nucleus. The PSTV experiments by Harders *et al.* (1989) used isolated purified nuclei and it is possible that the nucleolar concentration seen may be an artefact associated with the preparation of the nuclei. In view of our own results with CCCV, however, this distribution being purely artefactual is less likely, and some other explanation is therefore still required. Examination of the pattern of the distribution of signal for CCCV in the nucleolus in Figure 2(e) and (f) shows that the viroid sometimes forms short strings or clumps of signal, and is often concentrated towards the inner periphery of the nucleolar structure, as seen in Figure 2(e). The pattern of distribution of the viroid in Figure 2(e) is very similar to the patterns of rDNA gene transcription by RNA polymerase I as discussed in Highett *et al.* (1993a) and Shaw *et al.* (1995). Shaw et al. (1995) also noted that the central nucleolar vacuole, and the perinucleolar knobs are transcriptionally inactive zones. Both these structures are visible in the nucleolus shown in Figure 2(e), and they do not contain any significant amount of viroid signal. Shaw *et al.* (1995) concluded that the area of the nucleolus where they demonstrated transcription of the rDNA genes, which appears to be the same zone in which we found CCCV, comprising multiple fibrillar centres in a granular matrix surrounding a central vacuole, is where 'nascent and newly completed transcripts attached to and surrounding active genes' were located. The concentration of CCCV in this area could be interpreted as circumstantial evidence for the involvement of RNA polymerase I in the replication of CCCV. However, whether these patterns of viroid distribution, also seen in other tissue sections, are related to transcriptional or spliceosomal processes within the nucleolus, or are the result of viroids binding to other molecules that are involved in nucleolar transcription or splicing events, or even perhaps just to an accumulation of viroids at specific sites, is not known. We are, however, proceeding with experiments to see if viroids are associated with any of the known nucleolar-associated proteins.

There are precedents for the movement of small RNAs between the subnuclear compartments and even out into the cytoplasm and back again into the nucleus. The small

nuclear RNAs (snRNAs), especially the U RNAs which are complexed with proteins to become the snRNPs, or small ribonucleoproteins, are the nucleic acid components of the spliceosomes and are good examples of such mobile small RNAs. While some of these snRNAs are known to be synthesized in the nucleoplasm, their site of synthesis does not necessarily reflect their site of activity or known location (see Baserga and Steitz, 1993, and references therein). U8 RNA and U13 RNA are synthesized by RNA polymerase II in the nucleoplasm and are found in the nucleolus. The 5S and the 7S RNAs are synthesized by RNA polymerase III in the nucleoplasm, but are found in the nucleolus (Highett *et al.*, 1993b) and in the cytoplasm (Haas *et al.*, 1988), respectively.

The models published to date on the possible mechanisms of viroid pathogenicity are rather diverse. There are three related models that all draw on viroids having sequence homology to various positions on different snRNAs, including the 5′ end of U1 RNA from Novikoff hepatoma cells and some splice site junctions in pre-mRNA (Dickson, 1981), the internal transcribed sequence 2 (ITS2) in tomato, an intron-like sequence between the 5.8S and 28S rRNA (Jakab et al., 1986) and to the small domain of the 7S RNA in tomato (Haas *et al.*, 1988). Some sequence homologies between viroids and U RNAs from rat Novikoff hepatoma cells have been noted (Kiss and Solomosy, 1982, 1983), but as viroids are unique to plants, the exact relevance of these studies is not known. In another model, viroids are seen to bind to a double-stranded RNA-activated protein kinase and to alter the pattern of phosphorylation of this kinase protein (Diener *et al.*, 1993; Hiddinga *et al.*, 1988; Vera and Conejero, 1990). The common theme in all these papers is that the viroids (CEV and PSTV) exert their pathogenic effects by binding to, and thereby interfering with, the proper functioning of these snRNAs or proteins. In view of the varied models proposed in the papers discussed above, and our own results described here, we consider it possible that, if viroids do exert their pathogenic effects in this interfering manner, the binding of viroids to target snRNAs (or proteins) may be more general than previously thought. Different viroids may preferentially bind to different target molecules, or to the same target molecules at different sites, and this may also be the basis of the diverse host specificity seen between the different viroids.

Experimental procedures

Sample preparation for confocal microscopy

CEV. CEV extracted from infected tomato seedlings (kindly supplied by D. Warrilow) was used to infect tomato seedlings by manual inoculation of the cotyledons of 1-week-old plants. The tomato seedlings were grown in a growth chamber at 28°C with a 14 h daylight cycle. Samples of the leaves, petioles and roots of these plants and also of mock inoculated healthy control plants were taken at about 6 weeks of age when the symptoms of growth stunting, epinasty, leaf yellowing and necrosis were fully evident on the infected plants. Samples were cut into strips approximately 2–4 mm wide and up to 2 cm long. The samples were then fixed in 4% paraformaldehyde in 50 mM Pipes buffer, pH 7.6 at 4°C overnight on a rotator. The samples were then washed twice and taken to 70% ethanol prior to wax embedding in an automated processor (Shandon Citadel tissue processor).

CCCV. Tissue samples of CCCV-infected oil palm material and the healthy control samples were obtained as described in Bonfiglioli *et al.* (1994). Samples were taken from young (new) fronds and established fronds (approximately 2 months old) from glasshouse-grown plants that had been inoculated with gel-purified CCCV in 1984. Processing was the same as for CEV except that the fixation medium contained 1.5% nicotine to counteract the effects of the enzyme polyphenol oxidase (Koltunow, personal communication).

Sample preparation for electron microscopy.

CEV. Samples for electron microscopy were prepared from the same plants used for confocal microscopy specimens with the following modifications. Samples were cut to approximately 1×2 mm^2 and fixation was in 2.5% glutaraldehyde and 0.5% paraformaldehyde. A time-course study was done by taking samples from these plants weekly until 10 weeks of age when the plants began to die. The samples were embedded in LR Gold resin (London Resin Co.) and processed for electron microscopy as described in McFadden (1991).

CCCV. Processing for electron microscopy was as for CEV except for the addition of 1.5% nicotine in the fixation medium for reasons mentioned above.

Preparation of biotinylated cRNA probes

Biotinylated cRNA transcripts of approximately 250–350 nt in length corresponding to full-length positive and negative monomeric sequences of the different viroids were transcribed from viroid cDNA (McInnes *et al.*, 1989) cloned into the Bluescript transcription vector pBSK+ (Stratagene). Transcription was done according to the Promega Protocols and Applications Guide (Promega) with T7 or T3 RNA polymerase and the substitution of 60% of the UTP in the transcription mixture with biotin-11-UTP (Sigma Chemical Co). The transcription reactions (50 µl each) were diluted with transcription buffer (Promega) to 100 µl and unincorporated nucleotides were removed by centrifugation through a Bio-Spin 30 chromatography column (Bio-Rad). The cRNA transcripts were then precipitated by the addition of 2.5 volumes of ice-cold ethanol with ammonium acetate (pH 5.3) added to 300 mM and centrifuged at 14 000 r.p.m. in a refrigerated micro-centrifuge. The supernatant was removed and the transcripts were resuspended in 1 ml of *in situ* hybridization buffer (see McFadden, 1991) (50 mM Pipes buffer pH 7.4, 5 mM EDTA, 100 µg ml^{-1} of salmon sperm DNA, 0.14 M NaCl, 0.1% PVP 40, 0.1% Phycoll 400 and 50% de-ionized formamide). The insertion and linearization of the cDNA clones and transcription from them was done in such a way as to avoid the inclusion of the *Not*I site and other immediately adjacent sequences in the transcripts. The *Not*I site is a short, high GC content sequence in the middle of the polycloning site in pBSK+ that is reported (Witkiewicz *et al.*, 1993) to hybridize to some

ribosomal sequences and cause false positives in some low-temperature hybridization experiments (50°C or less).

In situ *hybridization for confocal laser scanning microscopy*

Sections of leaf material infected with the viroids and sections of uninfected leaf material of 5–8 μm thickness were cut from the wax blocks, floated on water and mounted on glass slides treated with silane (3-aminopropylsilane) (Sigma). Each individual slide contained sections of both infected and uninfected material. The slides were air dried and dewaxed by immersion in xylene for 5 min, and the xylene was then removed by immersion in 100% ethanol for a further 5 min. The slides were taken to 70% ethanol for 5 min, and then to water. The sections were digested with pepsin at 1 mg per ml in 50 mM glycine buffer (pH 3) for 12 min at room temperature, washed twice in 50 mM Tris–HCl, pH 7.4, 5 mM EDTA, dip washed in water, air dried, and then treated with RNase-free DNase (Boehringer) at 10 U per 100 μl in 50 mM Tris–HCl buffer (pH 7.4) overnight at 37°C; a coverslip was applied and the slides were placed in a humid chamber to prevent evaporation. Following overnight DNase digestion, the slides were washed twice in 50 mM Tris–HCl buffer (pH 7.4) containing 5 mM EDTA and then subjected to *in situ* hybridization. This was done by applying 100 μl of *in situ* hybridization buffer containing a range of dilutions of the RNA transcript probes on to different slides. Optimal dilutions of the probe were in the range of 1:250 to 1:500 in *in situ* hybridization buffer. The slides were then covered with a coverslip and the edges were liberally sealed with paraffin oil and the slide was placed on a 'slide griddle' (MJ Research) which was placed on top of a Thermal Cycler (MJ Research) and incubated at 65°C for 4 h to overnight. Following this incubation, the slides were cleaned by immersion in xylene for 5 min which removed the oil and also floated off the coverslip, then washed in 100% ethanol for 5 min, followed by 70% ethanol for 3 min and then washed in 2×SSC and 1×SSC for 45 min each at 42°C and then incubated in 0.2×SSC at 42°C for 30 min to remove any improperly hybridized or non-specifically bound probe. The slides were washed in water at room temperature for 3 min to remove salt and then air dried. Control experiments included the omission of the probe and omission of the fluorochrome as well as the use of healthy plant material. Omission of the probe is used to test for the presence of endogenous biotin as well as any other false signals.

Detection of biotinylated cRNA probes by confocal laser scanning microscopy

The biotinylated probes were localized by applying approximately 1 ml of 1:1000 dilution in phosphate buffered saline (PBS) of a stock solution (1 mg ml^{-1}) of the fluorescent dye Cy5 conjugated to strepavidin (Jackson Immunochemicals) and incubating for 1 h at room temperature. Cy5 is a far-red fluorochrome and was used because the fixed plant material in all specimens examined had high levels of autofluorescence in both the red and green channels. In the far-red channel, only very minimal autofluoresence was observed. The slides were then washed in PBS for 30 min followed by several washes in water and then counterstained by dipping in a solution of ethidium bromide (500 ng ml^{-1}) for 10 min. The ethidium bromide stains any undigested DNA as well as staining specifically for lignin in xylem skeletal elements (O'Brien and McCully, 1981). The data were collected in the green (autofluorescence used to show structural detail) and far-red (probe signal) wave bands of a Bio-Rad MRC 1000 confocal laser scanning microscope.

Electron microscopy

In situ hybridization for transmission electron microscopy using biotinylated cRNA probes, as well as the detection of these probes using 15 nm gold beads conjugated to strepavidin (Amersham) was done as described in Bonfiglioli *et al.* (1994).

Acknowledgements

This work was funded by the Australian Research Council Special Research Centre for Basic and Applied Plant Molecular Biology. We wish to thank David Warrilow for assistance with the CEV-infected tomato plants and for constructive discussions on the nature and functions of RNA polymerases. We also thank Dr Peter Kolesik for assistance with the confocal microscopy.

References

Baserga, S.J. and Steitz, J.A. (1993) The diverse world of small ribonucleoproteins. In *The RNA World* (Gestetland, R.F. and Atkins, J.F., eds). Cold Spring Harbor, NY: Cold Spring Harbor Laboratory Press, pp. 359–382.

Boccardo, G., Beaver, R.G., Randles, J.W. and Imperial, J.S. (1981) Tinangaja and bristle top, coconut diseases of uncertain etiology in Guam, and their relationship to cadang-cadang disease of coconut in the Phillipines. *Phytopathology*, **71**, 1104–1107.

Bonfiglioli, R.G., McFadden, G.I. and and Symons, R.H. (1994) *In situ* hybridisation localises avocado sunblotch viroid on chloroplast thylakoid membranes and coconut cadang cadang viroid in the nucleolus. *Plant J.* **6**, 99–104.

Bregman, D.B., Du, L., van der Zee, S. and Warren, S.L. (1995) Transcription-dependent redistribution of the large subunit of RNA polymerase II to discrete nuclear domains. *J. Cell Biol.* **129**, 287–298.

Da Graca, J.V. and Van Vuuren, S.P. (1981) Host range studies on avocado sunblotch. *South African Avocado Growers Assoc. Yearbook*, **4**, 81–82.

Dickson, E. (1981) A model for the involvement of viroids in RNA splicing. *Virology*, **115**, 216–221.

Diener, T.O. (1979) *Viroids and Viroid Diseases.* New York: John Wiley and Sons.

Diener, T.O., Hammond, R.W., Black, T. and Katze, M.G. (1993) Mechanism of viroid pathogenesis: differential activation of the interferon-induced, double-stranded RNA-activated, M,68 000 protein kinase by viroid strains of varying pathogenicity. *Biochimie*, **75**, 533–538.

Haas, B., Klanner, A., Ramm, K. and Sänger, H. (1988) The 7S RNA from tomato leaf tissue resembles a signal recognition particle RNA and exhibits remarkable sequence complementarity to viroids. *EMBO J.* **7**, 4063–4074.

Harders, J., Lukács.N., Robert-Nicoud, M., Jovin, T.M. and Riesner, D. (1989) Imaging of viroids from tomato leaf tissue by *in situ* hybridisation and confocal laser scanning microscopy. *EMBO J.* **8**, 3941–3949.

Haseloff, J., Mohamed, H.A. and Symons, R.H. (1982) Viroid RNAs of the cadang cadang disease of coconuts. *Nature*, **229**, 316–321.

Hendzel, M.J. and Bazett-Jones, D.P. (1995) RNA polymerase II transcription and the functional organization of the mammalian cell nucleus. *Chromosoma*, **103**, 509–516.

Hiddinga, H.J., Jessem Crum, C., Hu, J. and Roth, D. (1988) Viroid

induced phosphorylation of a host protein related to dsRNA dependent protein kinase. *Science*, **241**, 451–453.

Highett, M.I., Rawlins, D.J. and Shaw, P.J. (1993a) Different patterns of rDNA distribution in *Pisum sativum* nucleoli correlate with different levels of nucleolar activity. *J. Cell Sci.* **104**, 843–852.

Highett, M.I., Beven, A.F. and Shaw, P.J. (1993b) Localization of 5S genes and transcripts in *Pisum sativum* nuclei. *J. Cell Sci.* **105**, 1151–1158.

Jakab, G., Kiss, T. and Solomosy, F. (1986) Viroid pathogenicity and pre-rRNA processing: a model amenable to experimental testing. *Biochim. Biophys. Acta*, **868**, 190–197.

Keese, P. and Symons, R.H. (1985) Domains in viroids: Evidence of intermolecular RNA rearrangements and their contribution to viroid evolution. *Proc. Natl Acad. Sci. USA*, **82**, 4582–4586.

Keese, P., Osorio-Keese, M. and Symons, R.H. (1987) Coconut tinangaja viroid: Sequence homology with coconut cadang-cadang viroid and other potato spindle tuber viroid related RNAs. *Virology*, **162**, 508–510.

Keese, P., Visvader, J.E. and Symons, R.H. (1988) Sequence variability in plant viroid RNAs. In *RNA Genetics*, Volume III, Variability of RNA Genomes (Domingo, E., Holland, J.J. and Ahlquist, P., eds). Boca Raton, FL: CRC Press Inc., pp. 71–98.

Kirk, J.T.O. and Tilney-Bassett, R.A.E. (1978) *The Plastids: their Chemistry, Structure, Growth and Inheritance*, 2nd edn. Amsterdam: Elsevier/North Holland Biomedical Press, Chapters 7 and 9.

Kiss, T. and Solomosy, F. (1982) Sequence homologies between a viroid and a small nuclear RNA (snRNA) species of mammalian origin. *FEBS Lett.* **144**, 318–320.

Kiss, T. and Solomosy, F. (1983) Sequence homology between potato spindle tuber viroid and U3b snRNA. *FEBS Lett.* 163, 217–220.

Koltunow, A.M. and Rezaian, M.A. (1989) A scheme for viroid classification. *Intervirology*, **30**, 194–201.

Marcos, F. and Flores, R. (1992) Characterisation of RNAs specific to avocado sunblotch viroid synthesised *in vitro* by a cell-free system from infected avocado leaves. *Virology*, **186**, 481–488.

McFadden, G.I. (1991) *In situ* hybridisation techniques: molecular cytology goes ultrastructural. In *Electron Microscopy of Plant Cells* (Hall, J.M. and Hawes, C., eds). London: Academic Press, pp. 219–255.

McInnes, J.L., Habili, N. and Symons, R.H. (1989) Nonradioactive, photobiotin-labelled DNA probes for routine diagnosis of viroids in plant extracts. *J. Virol. Methods*, **23**, 299–312.

Mühlbach, H.P. and Sanger, H.L. (1979) Viroid replication is inhibited by α-amanitin. *Nature*, **278**, 185–188.

O'Brien, T.P. and McCully, M.E. (1981) *The Study of Plant Structure: Principles and Selected methods.* Melbourne: Termarcarphi Press.

Rivera-Bustamante, R.F. and Semancik, J.S. (1989) Properties of a viroid-replicating complex solubilised from nuclei. *J. Gen. Virol.* **70**, 2707–2717.

Scheer, U. and Rose, K. (1984) Localisation of RNA polymerase I in interphase cells and mitotic chromosomes by light and electron microscopic immuno-cytochemistry. *Proc. Natl Acad. Sci. USA*, **81**, 1431–1435.

Schindler, I.M. and Mühlbach, H.P. (1992) Involvement of nuclear DNA-dependent RNA polymerases in potato tuber spindle viroid replication: a reevaluation. *Plant Sci.* **84**, 221–229.

Schnell, D.J. and Blobel, G. (1993) Identification of intermediates in the pathway of protein import into chloroplasts and their localization to envelope contact sites. *J. Cell Biol.* **120**, 103–115.

Semancik, J.S. and Weathers, L.G. (1972) Exocortis disease: evidence for a new species of 'infectious' low molecular weight RNA in plants. *Nature (New Biol.)*, **237**, 242–244.

Semancik, J.S. and Vanderwoude, W.J. (1976) Exocortis viroid: cytopathic effects at the plasma membrane in association with pathogenic RNA. *Virology*, **69**, 719–726.

Shaw, P.J., Highett, M.I., Beven, A.F. and Jordan, E.G. (1995) The nucleolar architecture of polymerase I transcription and processing. *EMBO J.* **14**, 2896–2906.

Spiesmacher, E., Mühlbach, H.-P., Tabler, M. and Sänger, H.L. (1985) Synthesis of (+) and (–) RNA molecules of potato spindle tuber viroid (PSTV) in isolated nuclei and its impairment by transcription inhibitors. *Biosci. Rep.* **5**, 251–265.

Vera, P. and Conejero, V. (1990) Citrus exocortis viroid infection alters the *in vivo* pattern of protein phosphorylation of tomato leaf proteins. *Mol. Plant–Microbe Interact.* **3**, 28–32.

Wahn, K., Rosenberg-De Gomez, F. and Sänger, H.L. (1980) Cytopathic changes in leaf tissue of *Gynura aurantiaca* infected with the viroid citrus exocortis viroid. *J. Gen. Virol.* **49**, 355–365.

Witkiewicz, H., Bolander, M. and Edwards, D. (1993) Improved design of riboprobes from pBluescript and related vectors for *in situ* hybridisation. *Biotechniques*, **14**, 458–463.